This is a preprint, the final version is subject to change, of the American Mineralogist (MSA)
Cite as Authors (Year) Title. American Mineralogist, in press.
(DOI will not work until issue is live.) DOI: http://dx.doi.org/10.2138/am-2017-5727

Carbon as the dominant light element in the lunar core

Edgar S. Steenstra[1], Yanhao Lin[1], Nachiketa Rai[2,3], Max Jansen[1], Wim van Westrenen[1]

[1]Faculty of Earth and Life Sciences, Vrije Universiteit, Amsterdam, The Netherlands

[2]Centre for Planetary Sciences, Birkbeck–UCL, London, United Kingdom

[3]Department of Earth Sciences, Mineral and Planetary Sciences Division, Natural History Museum, London, United Kingdom

ABSTRACT

Geophysical and geochemical observations point to the presence of a light element in the lunar core, but the exact abundance and type of light element are poorly constrained. Accurate constraints on lunar core composition are vital for models of lunar core dynamo onset and demise, core formation conditions (e.g., depth of the lunar magma ocean or LMO) and therefore formation conditions, as well as the volatile inventory of the Moon. A wide range of previous studies considered S as the dominant light element in the lunar core. Here, we present new constraints on the composition of the lunar core, using mass balance calculations, combined with previously published models that predict the metal–silicate partitioning behavior of C, S, Ni and recently proposed new bulk silicate Moon (BSM) abundances of S and C. We also use the bulk Moon abundance of C and S to assess the extent of their devolatilization. We observe that the Ni content of the lunar core becomes unrealistically high if shallow (<3 GPa) LMO scenarios are assumed, and therefore only deeper (>3 GPa) LMO scenarios are considered for S and C. The moderately siderophile metal–silicate partitioning behavior of S during lunar core formation, combined with the low BSM abundance of S, yields only <0.16 wt% S in the core, virtually independent of the pressure (P) and temperature (T) conditions during core formation. Instead, our analysis suggests that C is the dominant light element in the lunar core. The siderophile behavior of C during lunar core formation

results in a core C content of ~0.6–4.8 wt%, with the exact amount depending on the core formation conditions. A C–rich lunar core could explain (1) the existence of a present–day molten outer core, (2) the estimated density of the lunar outer core and (3) the existence of an early lunar core dynamo driven by compositional buoyancy due to core crystallization. Finally, our calculations suggest the C content of the bulk Moon is close to its estimated abundance in the bulk silicate Earth (BSE), suggesting more limited volatile loss during the Moon-forming event than previously thought.

Keywords: Moon, Lunar, Core, Siderophile, Volatiles

INTRODUCTION

Geophysical and geochemical observations suggest the lunar core contains several wt% of one or more light elements. One constraint on the abundance and nature of the light element inventory stems from a reanalysis of Apollo era lunar seismograms suggesting the existence of a partially molten outer core (Weber et al. 2011), which requires the presence of one or more light elements to reduce the liquidus of the core. The existence of an ancient lunar core dynamo (e.g., Cisowski et al. 1983; Collinson 1993; Shea et al al. 2012) suggests the presence of one or more light elements in the lunar core, which is required to drive compositional convection in the lunar core (e.g., Laneuville et al. 2014). Light elements H, O and Si are not expected to significantly partition into the lunar core because the oxygen fugacity during lunar core formation was either too oxidizing (Si), or because the pressure in the Moon (~5 GPa at the core-mantle boundary, ~5.3 GPa in the center; Garcia et al. 2011, 2012) is too low (Killburn and Wood 1997; Ricolleau et al. 2011; Steenstra et al. 2016b).

From molten metal alloy density and liquidus considerations, Weber et al. (2011) proposed that the lunar core contains less than 6 wt% of lighter alloying elements. Sulfur (S) was deemed the most likely candidate, because of its high solubility in Fe metal, and its ability to

significantly reduce the bulk density, sound velocity and liquidus temperature of the lunar core (e.g., Hauck et al. 2006; Weber et al. 2011; Jing et al. 2014). Follow-up studies therefore primarily focused on assessing the feasibility of S in the lunar core. For example, Laneuville et al. (2013) suggested from thermochemical evolution models that ~3 wt% S would be required for the crystallization of a 240 km radius lunar inner core, whereas Zhang et al. (2013) propose lunar core S contents of ~5–10 wt%. Laneuville et al. (2014) proposed from thermochemical modeling of the lunar core dynamo an initial S core content of 7±1 wt%, or alternatively, more than 12 wt% if the Moon never crystallized an inner core. From Fe–S equation of state measurements, Jing et al. (2014) prefer a lunar core model with 4±3 wt% S, whereas Antonangeli et al. (2015) propose S core contents of 8.5±2.5 wt%, based on compressional and shear wave sound velocity and density measurements of γ–Fe at high pressures and temperatures. Rai and van Westrenen (2014) showed that the lunar mantle depletions of Cr and V can be explained by metal–silicate segregation of a lunar core containing 6 wt% S, if temperatures during core formation are limited to the lunar mantle liquidus. Steenstra et al. (2016b) showed that the depletions of 15 siderophile elements (including V and Cr) in the lunar mantle can also be explained at much lower S contents if super–liquidus temperatures during core formation are considered.

It is as of yet unclear how these proposed S contents of the lunar core relate to the lunar mantle or bulk silicate Moon (BSM) abundance of S. If single stage equilibrium between the lunar core and mantle occurred, which seems likely given the siderophile element depletion pattern in the lunar mantle (Rai and van Westrenen, 2014; Steenstra et al., 2016b), the proposed abundance of S in the lunar core must be compatible, at least to a reasonable extent, with the amount of S in the BSM.

From its siderophile behavior (Dasgupta et al. 2013; Chi et al. 2014) and its ability to significantly decrease both the Fe–metal liquidus and density relative to pure Fe (e.g., Chabot

et al. 2008; Sanloup et al. 2011) carbon (C) is another light element that could be present in the lunar core. However, the role of C was not quantitatively considered previously. Using recently proposed BSM abundances of C and S in conjunction with recently published models that describe their metal–silicate partitioning behavior as a function of pressure (*P*), temperature (*T*), composition of the silicate and metal (X) and oxygen fugacity (fO_2), here we re-assess the likelihood of one or both of these light elements are present in significant amounts in the lunar core. We also use these results to compare the lunar S and C inventories with their abundances in the bulk silicate Earth (BSE) to assess volatile loss from the Moon.

METHODS

We adopt a simple mass balance approach (e.g., Righter 2002) with which the amount of element *i* in the lunar core or mantle can be calculated (Eqs. 1, 2):

$$\mathrm{C}^{i}_{\mathrm{core}} = \mathrm{C}^{i}_{\mathrm{BM}} / \left[x_{core} + (1 - x_{core})/\mathrm{D(i)}\right] \quad (1)$$

$$\mathrm{C}^{i}_{\mathrm{mantle}} = \mathrm{C}^{i}_{\mathrm{BM}} / \left[x_{mantle} + (1 - x_{mantle}) * \mathrm{D(i)}\right] \quad (2)$$

in which C^i is defined as concentration of element *i* in the lunar core, $\mathrm{C}^{i}_{\mathrm{BM}}$ as the concentration by weight of element *i* in the bulk Moon (BM), *x* is either the core or lunar mantle mass fraction and D(i) is the metal–silicate partition coefficient D for element *i*. We calculate D(Ni, S, C) for three core formation scenarios detailed below (Table 1) by using the predictive models proposed by Rai and van Westrenen (2014), Boujibar et al. (2014) and Chi et al. (2014) for Ni, S and C, respectively. For each scenario, we calculate the amount of S and C at these *P*-*T* conditions and corresponding Ni contents.

Scenario 1 assumes a metal-silicate equilibration pressure during core formation of 3 GPa, corresponding to the presence during core formation of a lunar magma ocean with a depth of ~650 km. This depth corresponds to the depth from which deep moonquakes occur (>700 km, Nakamura et al., 1973), which could reflect the minimum original depth of the lunar magma ocean (Elkins-Tanton et al., 2011).

The maximum metal-silicate equilibration pressure of 4.8 GPa used in scenarios 2 and 3 is constrained by the estimated pressure at the core-mantle boundary (Garcia et al., 2011, 2012). These two scenarios therefore assume whole-Moon melting at the time of core formation. This seems plausible given the estimated disk midplane temperature (>3000-7000 K) derived from giant impact based lunar formation models (e.g., Canup, 2004; Nakajima and Stevenson, 2014; Hauri et al., 2015). Metal-silicate equilibration temperatures in whole-Moon melting models can range between the liquidus and the disk midplane temperature. Studies that linked the lunar mantle siderophile element depletions to their experimentally determined metal-silicate partitioning behavior also found that the Moon likely formed hot. Rai and van Westrenen (2014) found that the lunar mantle siderophile element depletions of Ni, Co, W, Mo, P, V, and Cr can be reconciled with formation of a <6 wt% S-bearing core in a fully molten Moon at liquidus temperatures. For scenarios 1 and 2, we therefore use the temperature ranges that are constrained by the lunar mantle liquidus parameterization proposed by Suckale et al. (2011) (Table 1). A follow up study of Steenstra et al. (2016b) extended this work and found that a lunar core with several wt% S is not required for the lunar mantle depletions of 15 siderophile elements if the lunar core formed at super-liquidus conditions in a fully molten Moon (T ~ 3150 ± 200 K). In scenario 3, we use the latter super-liquidus temperature range (Table 1).

The oxygen fugacity (fO_2) relative to the iron–wüstite buffer (ΔIW) is constrained to ΔIW = –2, a reasonable estimate given the FeO content of the lunar mantle (e.g., Rai and van

Westrenen 2014 and references therein). To quantify the possible silicate melt compositional effects on D(C, S, Ni), we consider an average of many recently proposed BSM compositions and corresponding *nbo/t* ratio of 2.55 in all three scenarios (Rai and van Westrenen, 2014) and references therein). Boujibar et al. (2014) and Chi et al. (2014) showed that the metal–silicate partitioning of S and C is dependent on the Ni content of the metal. We take this effect into account by calculating the predicted Ni content of the lunar core following each scenario, and using these Ni contents to calculate D(C, S) (Table 1). We therefore model either a Fe–Ni–S ($X_C^{met} = 0$) alloy or Fe–Ni–C ($X_S^{met} = 0$) alloy. We assume that no Si or O is dissolved in the lunar core (X_{Si}^{met} and $X_O^{met} = 0$). For C, our approach is validated by the negligible effect of up to 5 wt% S on D(C) (Li et al. 2015). However, D(S) has been shown to decrease with increasing C in the metal liquid (Boujibar et al. 2014). This would decrease D(S) if a C–rich lunar core would be considered. We will later show that the abundance of S in the lunar core is already very limited for a lunar core with $X_C^{met} = 0$, so we conclude that this effect will not change the outcome of our study.

The required BM abundances of C, S, and Ni are calculated with the derived metal–silicate partition coefficients (D's) and are combined with Eq. (3):

$$D_{mantle}^{core}(i) = [C_{BM}^{i} - x_{mantle} * C_{BSM}^{i}]/[C_{BSM}^{i} * (1 - x_{mantle})] \quad (3)$$

Rearranging yields Eq. (4):

$$C_{BM}^{i} = D_{mantle}^{core}(i) * C_{BSM}^{i} * (1 - x_{mantle}) + x_{mantle} * C_{BSM}^{i} \quad (4)$$

where $D_{mantle}^{core}(i)$ (or D(i)) is the required metal–silicate partition coefficient for element *i*, and C_{BSM}^{i} is the bulk silicate Moon (BSM) abundance of element *i*. The advantage of this

167 approach is that the outcome is independent of the assumed lunar core mass. We use the BSM
168 estimates of 470±50 ppm for Ni (Delano 1986), 74.5±4.5 ppm for S (Hauri et al. 2015; Chen
169 et al. 2015) and 54±10 ppm for C (Wetzel et al. 2015). Table 1 lists the *P–T* conditions during
170 lunar core formation that we explore in this study, as well as the calculated X_{Ni} content of the
171 lunar core at these conditions, used to calculate D(C, S).
172
173 **RESULTS**
174 **Nickel**
175 Nickel is considered as one of the major alloying elements in planetary cores, because of its
176 high abundance in primitive materials and its strongly siderophile tendencies at the *P–T-X–*
177 fO_2 conditions relevant for planetary differentiation. The metal–silicate partitioning behavior
178 of Ni as a function of *P–T–X–*fO_2 at lunar relevant conditions is well quantified (Rai and van
179 Westrenen 2014; Steenstra et al. 2016a, b) and mainly varies as a function of *P, T,* and fO_2.
180 The fO_2 during lunar core formation is well constrained to ~ΔIW = –2 by the FeO content of
181 the lunar mantle (e.g., Rai and van Westrenen 2014), leaving *P* and *T* as the dominant
182 variables affecting D(Ni) (Fig. 1). Due to the strong increase of D(Ni) with decreasing
183 temperature, we obtain unrealistically high Ni contents of the lunar core for shallow LMO
184 scenarios (<3 GPa) when using the Ni content of the lunar mantle of 470±50 ppm (Delano
185 1986). For example, core–mantle equilibration at 1 GPa would have resulted in an lunar Ni
186 core content of >56 wt%. In the following calculations, we therefore focus on scenarios where
187 the LMO equilibrated with the lunar core at depths greater than ~650 km (corresponding to *P*
188 >3 GPa). We note that a deep LMO is also suggested from a wide range of other siderophile
189 element depletions in the lunar mantle (Rai and van Westrenen 2014; Steenstra et al. 2016b).
190
191

192 **Sulfur**

193 Recent analyses of a wide range of lunar volcanic glasses (Hauri et al. 2015) and various lunar
194 melt inclusions (Chen et al. 2015) suggest that the BSM contains 74.5±4.5 ppm of sulfur. The
195 predictive equation for log D(S) provided by Boujibar et al. (2014) suggests that the metal–
196 silicate partitioning behavior of S at lunar relevant conditions mainly varies as a function of *P*,
197 the FeO content of the lunar mantle and the Ni content of the lunar core (Fig. 1). For each of
198 the three scenarios, we calculate an overall log D(S) range of ~0.25–1.30. Using the BSM
199 estimates of Chen et al. (2015) and Hauri et al. (2015), this corresponds to BM abundances
200 ranging between ~71–116 ppm S, somewhat lower than the estimated bulk silicate Earth
201 (BSE) content of 250±50 ppm S (McDonough and Sun 1995). Using a BM abundance of
202 ~71–116 ppm S, the resulting lunar core S content is only ~0.01–0.16 wt%, with the exact
203 amount depending of the scenario considered (Table 1). An example is given in Fig. 2a,
204 where the estimated lunar core and mantle S content is calculated if scenario 2 is considered.
205 The maximum S core content (~0.14±0.02 wt%) is expected for a deep LMO with super–
206 liquidus temperatures (scenario 3), whereas assuming an intermediate depth LMO (3 GPa,
207 scenario 1) and corresponding liquidus temperatures, would result in even lower S content
208 (0.02±0.01 wt%). An important observation is the minor variation in estimated core S content,
209 across a wider range of log D(S) values (Table 2). We conclude that the calculated lunar core
210 S abundances are close to 2 orders of magnitude lower than those proposed from other studies
211 (e.g., Weber et al. 2011; Jing et al. 2014; Laneuville et al. 2013, 2014; Antonangeli et al.
212 2015) irrespective of core formation conditions.
213

214 **Carbon**

215 Recent high–precision measurements of indigenous C contents in primitive lunar volcanic
216 glasses and melt inclusions, combined with solubility and degassing model calculations,

217 suggest that the BSM contains 54±10 ppm C (Wetzel et al. 2015). The metal–silicate
218 partitioning behavior of C has been shown to be strongly dependent on *P, T,* fO_2 and silicate
219 melt composition, approximated with parameter *nbo/t* in this study (Dasgupta et al. 2013; Chi
220 et al. 2014; Li et al. 2015). At the conditions relevant for lunar core formation, this results in
221 relatively siderophile behavior of C, relative to S (Fig. 1). We calculate an overall lunar core
222 C content range of ~0.6–4.8 wt%, with the exact amount dependent of the core formation
223 scenario considered (Table 1). An example of such a calculation is shown in Fig. 2b. The
224 maximum lunar core C content (3.6±1.2 wt%) is expected for scenario 2. For a deep LMO
225 with super–liquidus conditions, the C core content is reduced to ~2.2±0.9 wt% and for an
226 intermediate depth LMO to ~1.1±0.5 wt% (Table 2). We conclude that in all scenarios C has
227 strongly siderophile behavior, resulting in C being a feasible candidate for the light element in
228 the lunar core. We calculate a range of ~740±520 ppm C in the bulk Moon. This range is in
229 perfect agreement with the estimated C content of the BSE of ~765±300 ppm C (Marty 2012),
230 emphasizing the similarity between the BM and BSE (e.g., de Meijer et al. 2013) and the
231 apparent minor extent of devolatilization depletion of the Moon relative to BSE.
232

233 ## DISCUSSION

234 ### Uncertainty in bulk silicate Moon estimates

235 One potential source of error in our models is uncertainty in the assumed BSM abundances
236 of S and C. For example, the concentration of S and C in lunar rocks could have been affected
237 by devolatilization processes on the Moon after lunar core formation. One way to assess the
238 loss of S following core formation is to study the S isotope compositions of lunar basalts.
239 Wing and Farquhar (2015) measured the S isotope compositions for a wider range of lunar
240 mare basalts, including primitive (low–Ti) mare basalts, and suggest only 1–10 % of S was
241 lost due to degassing processes. This range falls largely within the error bars on the BSM

242 estimate for S that we consider here. Moreover, three independent studies report very similar
243 S contents of the BSM (Bombardieri et al. 2005; Chen et al. 2015; Hauri et al. 2015) for a
244 variety of lunar sample types. Another potential issue is the crystallization of sulfides, through
245 which S (and other siderophile elements, such as C) could be removed from mare basalts prior
246 to eruption. However, Bombardieri et al. (2005) found no evidence for sulfide saturation of
247 the mare basalts. Unless the mare basalts experienced significant S loss, which is not recorded
248 in the S isotope composition of the lunar basalts, sulfide saturation cannot have occurred.
249 We also note that even if the primitive BSM concentrations of S and C are significantly
250 underestimated, the general outcome of this study will not change. For example, assuming a
251 BSM abundance of 300 ppm S, corresponding to the upper estimate for the BSE, would still
252 result in less than ~0.6 wt% S in the lunar core. On the contrary, assuming a slightly higher
253 BSM for C drastically increases its abundance in the lunar core. For example, 80 ppm C in the
254 lunar mantle would result in a lunar core C content of ~1.3–6.0 wt% C, emphasizing the
255 geochemical feasibility of C as the dominant light element in the lunar core. The overall
256 conclusion that C should be far more abundant in the lunar core than S is also robust.
257

258 **Comparison with geophysical observations**

259 The presence of a specific light element in the lunar core should also be compatible with
260 geophysical observations. Density, sound velocity and physical state of the lunar core may
261 provide valuable constraints on lunar core composition. Weber et al. (2011) and other recent
262 studies of the geophysical properties of the lunar outer core suggest V_p values of 4.1±0.2 km/s
263 (Weber et al. 2011; Jing et al. 2014). Unfortunately, the physical parameters (e.g., Gruneisen
264 parameter, shear modulus, thermal expansivity) of Fe–C liquids are poorly constrained, which
265 prohibits a quantitative assessment. However, C is known to lower V_p relative to pure Fe due
266 to its effect on lowering the density and bulk modulus of Fe–alloys, similar to S. Another

267 important proxy for the nature of the light element in the lunar outer core is density. The
268 density of the lunar outer core was constrained by Weber et al. (2011) to ~5.1 g/cm^3.
269 However, from sound velocity data of Fe–FeS liquids Jing et al. (2014) suggest the lunar
270 outer core is much denser (~6.5±0.5 g/cm^3), whereas Antonangeli et al. (2015) propose a
271 lunar outer core density of ~5.25±1.75 g/cm^3 based on compressional and shear wave sound
272 velocity and density measurements of γ–Fe. These ranges illustrate the major uncertainty in
273 the lunar outer core density. It is noteworthy to mention that the estimated density ranges of
274 liquid Fe + 5.7 wt% C and liquid Fe + 3.5 wt% C at 5 GPa (Sanloup et al. 2011; Shimoyama
275 et al. 2013), based on X–ray absorption techniques, fall within or are close the latter density
276 ranges. We also note that that the density of Fe–C and Fe–S melts, at identical pressure and
277 temperature (4 GPa, 1923 K) do not show significant differences, except for very S rich
278 compositions (Shimoyama et al. 2013), which is ruled out from low BSM abundances of S.
279 Like S, C also significantly decreases the liquidus temperatures of Fe alloys (e.g., Chabot
280 et al. 2008). For example, the liquidus temperature for the Fe–C eutectic composition is
281 ~1500±25 K at 5 GPa (Chabot et al. 2008) relative to ~2000 K for pure Fe and ~1260±25 K at
282 6 GPa for Fe-S (Buono and Walker 2011). The presence of C in the lunar core could therefore
283 explain the partially molten state of the lunar outer core (Weber et al. 2011).
284 Finally, an important constraint on the light element composition of the lunar core is the
285 former existence of a lunar core dynamo. If we assume the lower boundary for the present-
286 day core-mantle boundary temperature of ~1650 K (Weber et al. 2011; Antonangeli et al.
287 2015), required for the presence of a partial silicate melt layer at the lunar core–mantle
288 boundary, γ–Fe would crystallize at C contents below ~3.8 wt% and could form the inner
289 core. This could lead to compositional heterogeneity and buoyancy in the outer core, which
290 can help to initiate and sustain an early lunar core dynamo (Chabot et al. 2008). A Fe_3C inner
291 core seems unlikely given the solubility limit of C of ~6 wt% in Fe-Ni melts at these

conditions (Chi et al. 2014), as well as from sound velocity measurements of the lunar inner core (Antonangeli et al. 2015). The errors on the geophysical lunar interior structure properties discussed here are substantial, even with the new data obtained from the SELENE (Selenological and Engineering Explorer or Kaguya) and GRAIL (Gravity Recovery and Interior Laboratory) missions (Yamada et al. 2014). Overall, we conclude that from current geophysical constraints, a C-rich lunar core needs to be seriously considered.

IMPLICATIONS

This work suggests from geochemical considerations that C should be the dominant light element in the lunar core, given its highly siderophile tendencies and high abundance in the BSM. This results in an estimated C core content range of ~0.6–4.8 wt% for a wider range of core formation scenarios. This demonstrates the geochemical feasibility of a C-rich lunar core, instead of a S-rich lunar core as previously suggested. In addition, given the amount of S in the lunar core we calculate here (<0.16 wt% S across a wider range of core–mantle equilibration scenarios), it would be difficult to maintain a partially molten core over a long temperature/time interval without another or additional light elements. A C–rich core would explain (1) the present day molten lunar outer core, (2) the suggested density deficit of the lunar outer core and possibly (3) the existence of a (partly) compositionally driven core dynamo through crystallization of Fe metal. Our hypothesis of a C-rich lunar core can be tested by (1) additionally constraining the physical properties of Fe–C liquids at lunar relevant conditions, (2) numerically assessing the feasibility of a lunar core dynamo for a C–rich lunar core and (3) assessing if the siderophile element depletions in the lunar mantle can be reconciled with metal–silicate segregation of a C–rich lunar core. Finally, we note that the BM estimates derived in this study for S and C are relatively close to the estimated BSE abundances of these elements, which confirms once again the close compositional similarities

317 between the BM and BSE, as well as the lack of significant devolatilization during the Moon–
318 forming event. This conclusion is consistent with recent observations for other volatile
319 elements, e.g., H_2O (Hauri et al. 2015) and a wide range of volatile siderophile elements
320 (Steenstra et al. 2016b).
321

322 **ACKNOWLEDGEMENTS**

323 We would like to acknowledge the constructive feedback from two anonymous reviewers, and
324 thank H. Watson for her editorial handling of the manuscript. This study was funded by a
325 Netherlands Organisation for Scientific Research (N.W.O.) Vici grant to WvW. We
326 acknowledge fruitful discussions with P. Kaskes and S. de Graaff. We would also like to
327 thank A. Boujibar for providing calculation details of her published work. ESS would like to
328 thank the Planetary Science Institute (PSI) for financial support through the 2015 Pierazzo
329 International Student Travel Award.
330

331 **REFERENCES CITED**

332 Antonangeli, D., Morard, G., Schmerr, N.C., Komabayashi, T., Krisch, M., Fiquet, G., and
333 Fei, Y. (2015) Towards a mineral physics reference model for the Moon's core.
334 Proceedings of the National Academy of Sciences, 112, 3916–3919.
335 Bombardieri, D.J., Norman, M.D., Kamenetsky, V.S. and Danyushevsky, L.V. (2005) Major
336 element and primary sulfur concentrations in Apollo 12 mare basalts: The view from melt
337 inclusions. Meteoritic and Planetary Science, 40, 679–693.
338 Boujibar, A., Andrault, D., Bouhifd, M.A., Bolfan–Casanova, N., Devidal, J.–L., and Trcera,
339 N. (2014) Metal–silicate partitioning of sulphur, new experimental and thermodynamic
340 constraints on planetary accretion. Earth and Planetery Science Letters, 391, 42–54.

341 Buono, A.S., and Walker, D. (2011) The Fe–rich liquidus in the Fe–FeS system from 1 bar to
342 10 GPa. Geochimica et Cosmochimica Acta, 75, 2072–2087.
343 Canup, R. M. (2004). Simulations of a late lunar-forming impact. Icarus, 168, 433-456.
344 Chabot, N.L., Campbell, A.J., McDonough, W.F., Draper, D.S., Agee, C.B., Humayun, M.,
345 Watson, H.C., Cotrell, E., and Saslow, S.A. (2008) The Fe–C system at 5 GPa and
346 implications for Earth's core. Geochimica et Cosmochimica Acta, 72, 4146–4158.
347 Chen, Y., Zhang, Y., Liu, Y., Guan, Y., Eiler, J., and Stolper, E.M. (2015) Water, fluorine,
348 and sulfur concentrations in the lunar mantle. Earth and Planetary Science Letters, 427,
349 37–46.
350 Chi, H., Dasgupta, R., Duncan, M.S., and Shimizu, N. (2014) Partitioning of carbon between
351 Fe–rich alloy melt and silicate melt in a magma ocean – implications for the abundance
352 and origin of volatiles in Earth, Mars, and the Moon. Geochimica et Cosmochimica Acta,
353 139, 447–471.
354 Cisowski, S.M., Collinson, D.W., Runcorn, S.K., and Stephenson, A. (1983) A review of
355 lunar paleointensity data and implications for the origin of lunar magnetism. Journal of
356 Geophysical Research, 88, A691–A704.
357 Collinson, D.W. (1993) Magnetism of the Moon – A lunar core dynamo or impact
358 magnetization? Surveys in Geophysics, 14, 89–118.
359 Dasgupta, R., Chi, H., Shimizu, N., Buono, A.S., and Walker, D. (2013) Carbon solution and
360 partitioning between metallic and silicate melts in a shallow magma ocean: Implications
361 for the origin and distribution of terrestrial carbon. Geochimica et Cosmochimca Acta,
362 102, 191–212.
363 de Meijer, R.J., Anisichkin, V.F., and van Westrenen, W. (2013) Forming the Moon from
364 terrestrial silicate–rich material. Chemical Geology, 345, 40-49.

Delano, J.W. (1986) Abundances of cobalt, nickel, and volatiles in the silicate portion of the Moon. In W.K. Hartmann, R.J. Phillips, G.J. Taylor, Eds., Origin of the Moon, Lunar and Planetary Institute, Houston (1986), p.231–248.

Elkins-Tanton, L.T., Burgess, S., Yin, Q.-Z. (2011) The lunar magma ocean: Reconciling the solidification process with lunar petrology and geochronology. Earth and Planetary Science Letters, 304, 326-336.

Garcia, R.F., Gagnepain-Beyneix, J., Chevrot, S., Lognonné, P. (2011) Very preliminary reference Moon model. Physics of the Earth and Planetary Interiors, 202-203, 89-91.

Garcia, R.F., Gagnepain-Beyneix, J., Chevrot, S., Lognonné, P. (2012) Erratum to ''Very preliminary reference Moon model. Physics of the Earth and Planetary Interiors, 202-203, 89-91.

Hauck, S.A., Aurnou, J.M., and Dombard A.J. (2006) Sulfur's impact on core evolution and magnetic field generation on Ganymede. Journal of Geophysical Research: Planets, 111, E09008, doi:10.1029/2005JE002557.

Hauri, E.H., Saal, A.E., Rutherford, M.J., and van Orman, J.A. (2015) Water in the Moon's interior: Truth and consequences. Earth and Planetary Science Letters, 409, 252–264.

Jing, Z., Wang, Y., Kono, Y., Yu, T., Sakamaki, T., Park, C., Rivers, M.L., Sutton, S.R., and Shen, G. (2014) Sound velocity of Fe–S liquids at high pressure: Implications for the Moon's molten outer core. Earth and Planetary Science Letters, 396, 78–87.

Killburn, M.R., and Wood, B.J. (1997) Metal–silicate partitioning and the incompatibility of S and Si during core formation. Earth and Planetary Science Letters, 152, 139–148.

Laneuville, M., Wieczorek, M.A., Breuer, D., and Tosi, N. (2013) Asymmetric thermal evolution of the Moon. Journal of Geophysical Research: Planets, 118, 1435–1452.

Laneuville, M., Wieczorek, M.A., Breuer, D., Aubert, J., Morard, G., and Rückriemen, T. (2014) A long–lived lunar dynamo powered by core crystallization. Earth and Planetary Science Letters, 401, 251–260.

Li, Y., Dasgupta, R., and Tsuno, K. (2015) The effects of sulfur, silicon, water, and oxygen fugacity on carbon solubility and partitioning in Fe–rich alloy and silicate melt systems at 3 GPa and 1600° C: Implications for core–mantle differentiation and degassing of magma oceans and reduced planetary mantles. Earth and Planetary Science Letters, 415, 54–66.

Marty, B. (2012) The origins and concentrations of water, carbon, nitrogen and noble gases on Earth. Earth and Planetary Science Letters, 313–314, 56–66.

McDonough, W.F., and Sun, S.–s. (1995) The composition of the Earth. Chemical Geology, 120, 223–253.

Nakajima, M., Stevenson, D.J. (2014). Investigation of the initial state of the Moon-forming disk: bridging SPH simulations and hydrostatic models. Icarus, 233, 259-267.

Nakamura, Y., Lammlein, D., Latham, G., Ewing, M., Dorman, J., Press, F., Toksöz, N. (1973) New seismic data on state of deep lunar interior. Science, 181, 49-51.

Rai, N., and van Westrenen, W. (2014) Lunar core formation: New constraints from metal–silicate partitioning of siderophile elements. Earth and Planetary Science Letters, 388, 343–352.

Ricolleau, A., Fei ,Y., Corgne, A., Siebert, J., and Badro, J. (2011) Oxygen and silicon contents of the Earth's core from high pressure metal–silicate partitioning experiments. Earth and Planetary Science Letters, 310, 409–421.

Righter, K. (2002) Does the Moon Have a Metallic Core?: Constraints from Giant Impact Modeling and Siderophile Elements. Icarus, 158, 1–13.

411 Sanloup, C., van Westrenen, W., Dasgupta, R., Maynard-Casely, H., Perrillat, J.-P. (2011)
412 Compressibility change in iron-rich melt and implications for core formation models.
413 Earth and Planetary Science Letters, 306, 118-122.
414 Shea, E.K., Weiss, B.P., Cassata, W.S., Shuster, D.L., Tikoo, S.M., Gattacceca, J., Grove,
415 T.L., Fuller, M.D. (2012) A Long-Lived Lunar Core Dynamo. Science, 335, 453-456.
416 Shimoyama, Y., Terasaki, H., Ohtani, E., Urakawa, S., Takubo, Y., Nishida, K., Suzuki, A.,
417 and Katayama, Y. (2013) Density of Fe–3.5 wt.% C liquid at high pressure and
418 temperature and the effect of carbon on the density of the molten iron. Physics of the
419 Earth and Planetary Interiors, 224, 77–82.
420 Suckale, J., Elkins–Tanton, L.T., and Sethian, J.A. (2012) Crystals stirred up: 2. Numerical
421 insights into the formation of the earliest crust on the Moon. Journal of Geophysical
422 Research, 117, E08005.
423 Steenstra, E.S., Knibbe, J.S., Rai, N., and van Westrenen, W. (2016a) Constraints on core
424 formation in Vesta from metal–silicate partitioning of siderophile elements. Geochimica et
425 Cosmochimica Acta, 177, 48-61.
426 Steenstra, E.S., Rai, N., Knibbe, J.S., Lin, Y.H, and van Westrenen, W. (2016b) New
427 geochemical models of core formation in the Moon from the metal–silicate partitioning of
428 15 siderophile elements. Earth and Planetary Science Letters, 441, 1-9.
429 Weber, R.C., Lin, P–Y., Garnero, E.J., Williams, Q., and Lognonné, P. (2011) Seismic
430 Detection of the Lunar Core. Science, 331, 309–312.
431 Wetzel, D.T., Hauri, E.H., Saal, A.E., and Rutherford, M. J. (2015) Carbon content and
432 degassing history of the lunar volcanic glasses. Nature Geoscience, 8, 755–758.
433 Wing B.A., and Farquhar, J. (2015) Sulfur isotope homogeneity of lunar mare basalts.
434 Geochimica et Cosmochimica Acta, 170, 266–280.

Yamada, Y., Matsumoto, K., Kikuchi, F., Sasaki, S. (2014) Error determination of lunar interior structure by lunar geodetic data on seismic restriction. Physics of the Earth and Planetary Interiors, 231, 56-64.

Zhang, N., Parmentier, E.M., and Liang, Y. (2013) A 3–D numerical study of the thermal evolution of the Moon after cumulate mantle overturn: The importance of rheology and core solidification. Journal of Geophysical Research: Planets, 118, 1789–1804.

Figure captions

Figure 1. The modeled partitioning behavior of C, S, and Ni along the *P* and corresponding solidus–liquidus *T* range (Suckale et al. 2012) relevant for the lunar interior, assuming ΔIW = –2, *nbo/t* = 2.55, and X_{Ni} = 0.20 for D(C, S). D(C, S, Ni) were modeled using predictive equations from Boujibar et al. (2014) for S, Chi et al. (2014) for C, and Rai and van Westrenen (2014) for Ni.

Figure 2. The expected abundance of light elements in the lunar core or mantle, as a function of bulk Moon (BM) abundance, assuming ΔIW = –2, *P* = 4.8 GPa, *T* = 2250 K, *nbo/t* = 2.55 and X_{Ni} = 0.21±0.02, calculated using Eqs. (1–4) and the predictive models for D(S) of Boujibar et al. (2014) and D(C) of Chi et al. (2014). Panel (a) shows the results for S, with the horizontal lines representing the BSM estimates from Bombardieri et al. (2005), Chen et al. (2015) and Hauri et al. (2015) and vertical lines the range of corresponding BM abundances. Panel (b) shows the estimated lunar core and mantle content for C, with the horizontal lines representing the BSM estimate from Wetzel et al. (2015) and vertical lines the lower and upper limit of the BM abundance. Also displayed is the estimated carbon solubility limit in Fe–rich melts derived from Chi et al. (2014).

460 **Table 1** Modeled *P–T* conditions with corresponding log D(Ni, S, C), resulting mole fraction of Ni in the lunar core, and estimated abundances

461 (ppm or wt%) of carbon and sulfur in the lunar core, assuming fO_2 of ΔIW = –2 and *nbo/t* = 2.55

Scenario	P (GPa)	T (K)	Nickel (Ni)		Sulfur (S)			Carbon (C)		
			Log D [1]	X_{Ni}	Log D [3]	BM (ppm)	Core (wt%)	Log D [4]	BM (ppm)	Core (wt%)
1) Intermediate LMO	3.0	2150	2.88	0.34±0.04	0.46±0.21	79±8	0.02±0.01	2.30±0.10	331±137	1.11±0.51
2) Deep LMO [1]	4.8	2250	2.67	0.21±0.02	1.17±0.08	101±12	0.11±0.03	2.82±0.05	951±303	3.59±1.17
3) Deep LMO [2]	4.8	3150±200	2.45±0.04	0.13±0.03	1.26±0.03	107±9	0.14±0.02	2.60±0.07	598±225	2.18±0.86

462 [1] Rai and van Westrenen (2014), liquidus temperature [2] Steenstra et al. (2016b), superliquidus temperature [3] Boujibar et al. (2014) [4] Chi et al. (2014)

463

464

465

466

467

468

469

470

471

472

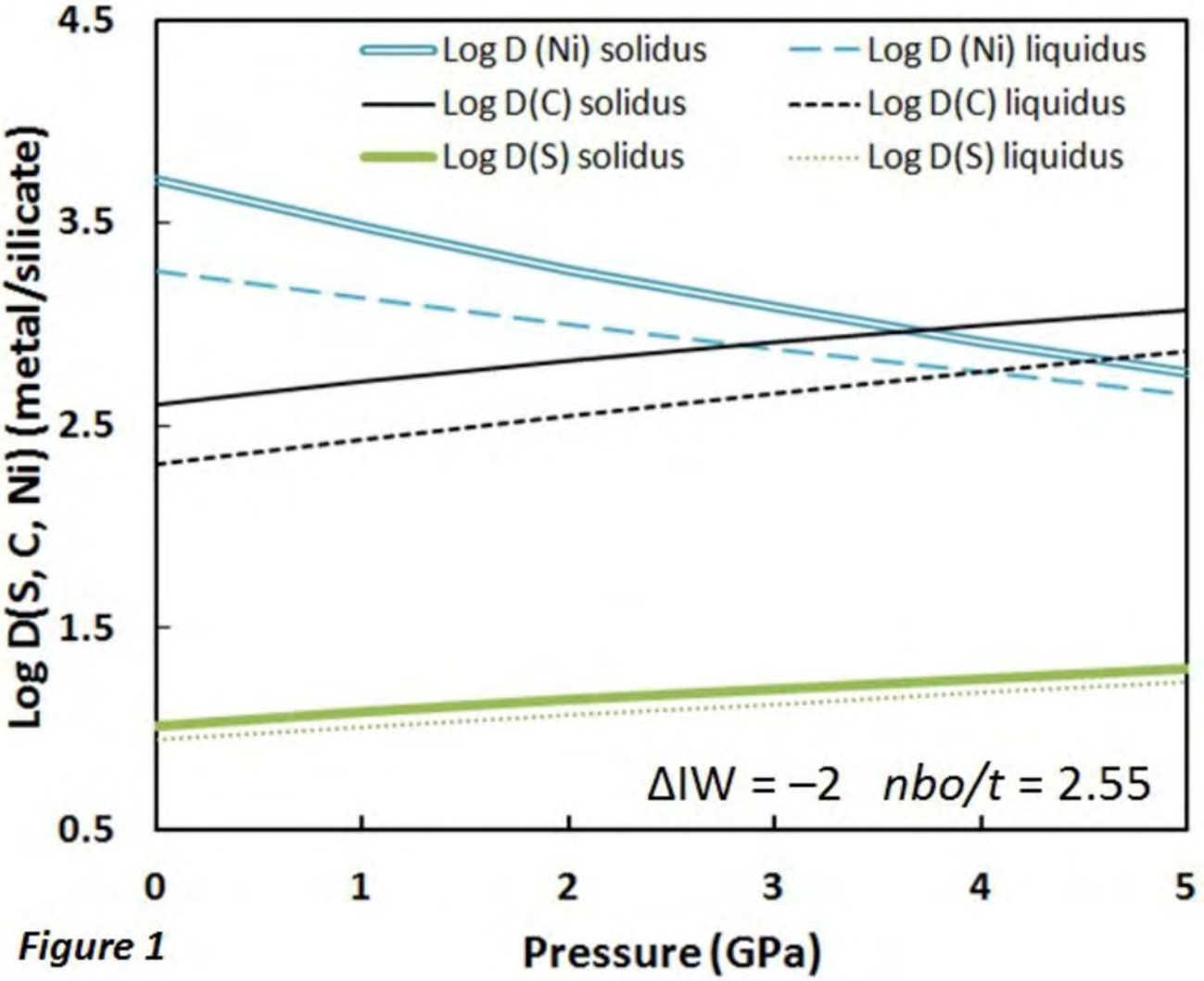
Log D (Ni) solidus
Log D (Ni) liquidus
Log D(C) solidus
Log D(C) liquidus
Log D(S) solidus
Log D(S) liquidus
ΔIW = –2 nbo/t = 2.55
Log D(S, C, Ni) (metal/silicate)
Pressure (GPa)
4.5
3.5
2.5
1.5
0.5
0
1
2
3
4
5

Figure 1

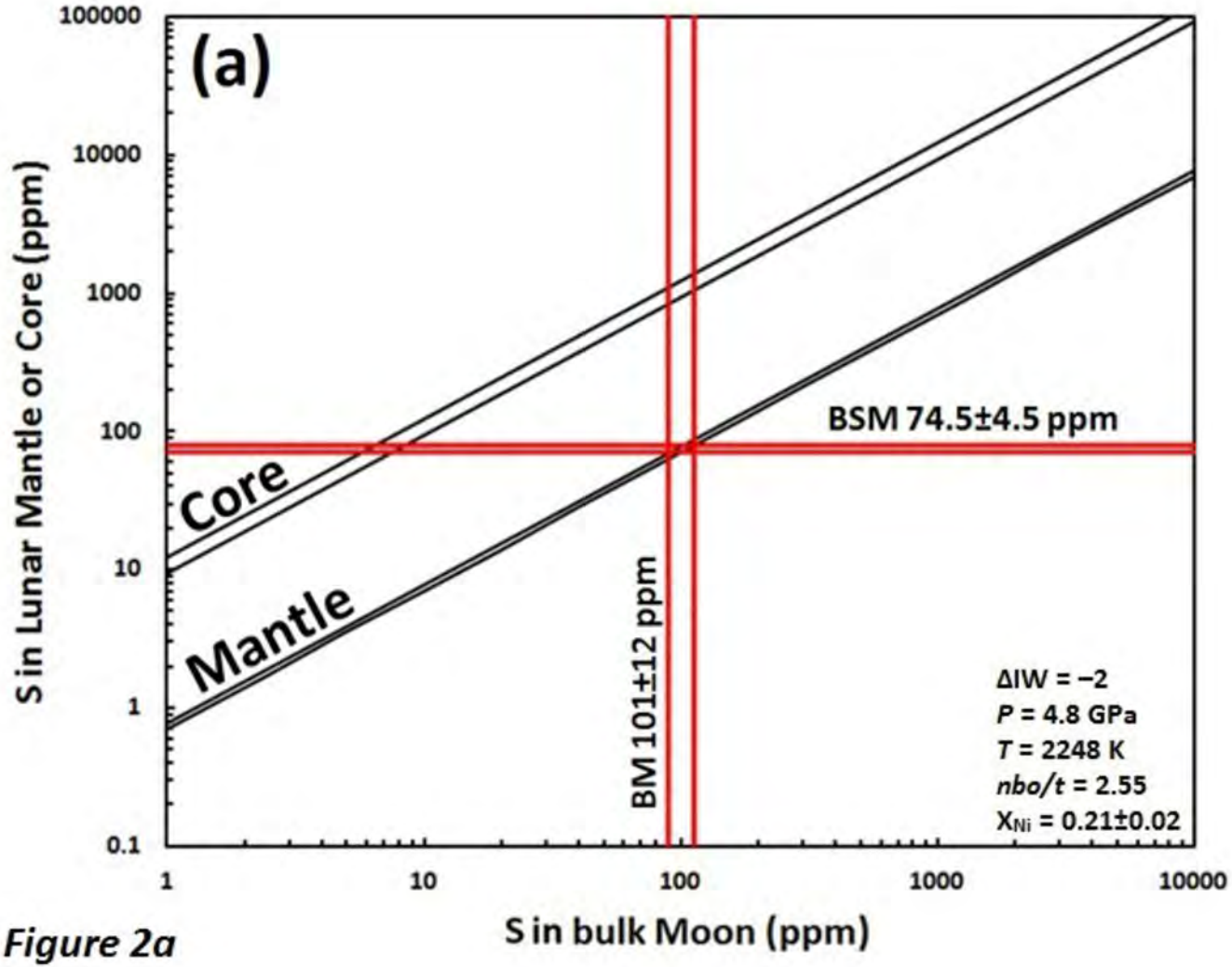
(a)
100000
10000
1000
100
10
1
0.1
S in Lunar Mantle or Core (ppm)
Core
Mantle
BSM 74.5±4.5 ppm
BM 101±12 ppm
ΔIW = −2
P = 4.8 GPa
T = 2248 K
nbo/t = 2.55
X_Ni = 0.21±0.02
1
10
100
1000
10000
S in bulk Moon (ppm)

Figure 2a

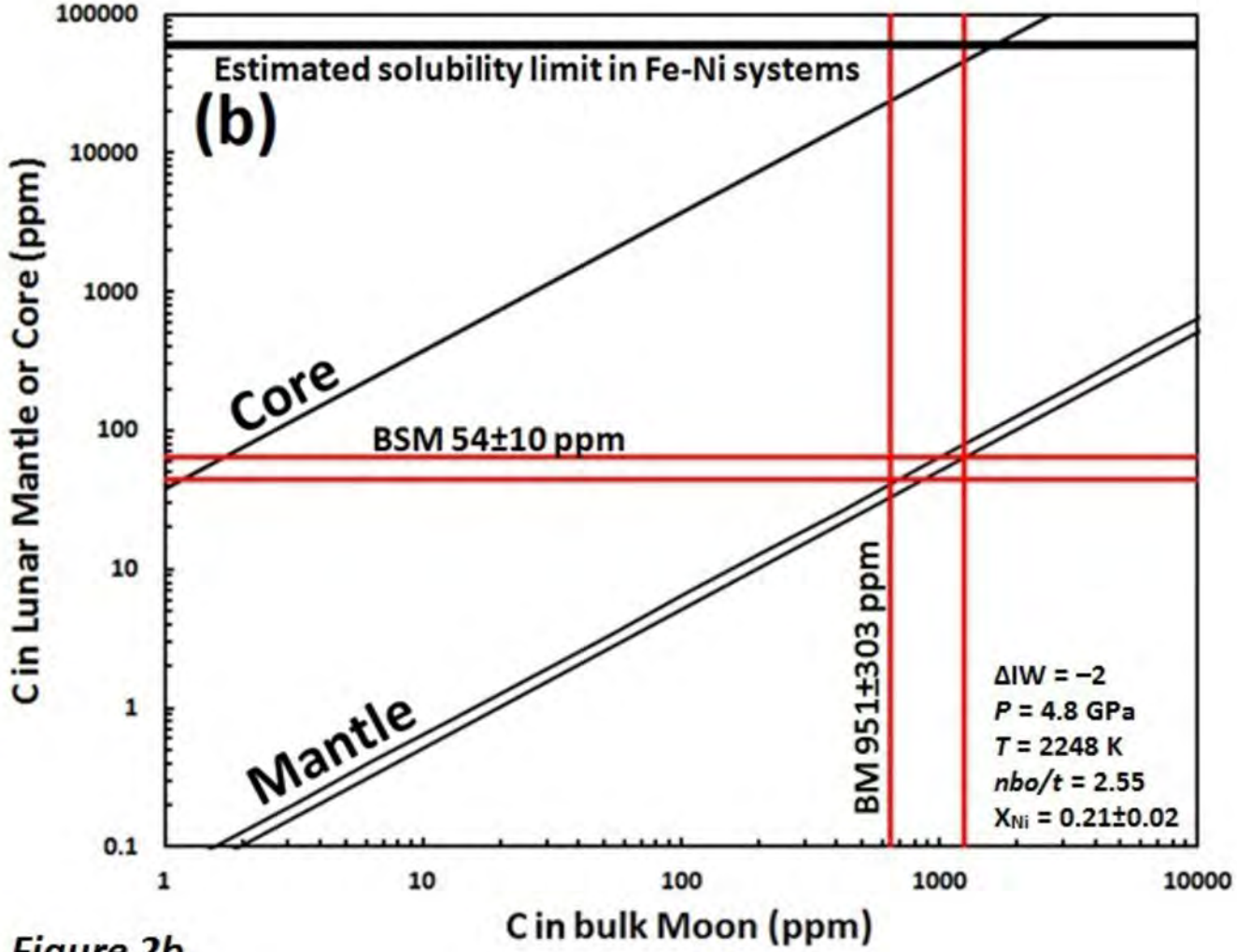
Estimated solubility limit in Fe-Ni systems
(b)
Core
BSM 54±10 ppm
Mantle
BM 951±303 ppm
ΔIW = −2
P = 4.8 GPa
T = 2248 K
nbo/t = 2.55
X_Ni = 0.21±0.02
C in Lunar Mantle or Core (ppm)
C in bulk Moon (ppm)
100000
10000
1000
100
10
1
0.1
1
10
100
1000
10000

Figure 2b